JTTEE5 15:676-681
DOI: 10.1361/105996306X147072
1059-9630/$19.00 © ASM International

Peer Reviewed

Suspension Plasma Spraying of Nanostructured WC-12Co Coatings

J. Oberste Berghaus, B. Marple, and C. Moreau

(Submitted February 27, 2006; in revised form April 19, 2006)

Nanostructured WC-12% Co coatings were deposited by suspension plasma spraying of submicron feedstock powders, using an internal injection plasma torch. The liquid carrier used in this approach allows for controlled injection of much finer particles than in conventional thermal spraying, leading to thin coatings with a fine surface finish. A polyethylene-imine (PEI) dispersant was used to stabilize the colloidal suspension in an ethanol carrier. In-flight particle states were measured for a number of operating conditions of varying plasma gas flow rates, feed rates, and standoff distances and were related to the resulting microstructure, phase composition (EDS, SEM, XRD), and Vickers hardness. High in-flight particle velocities (>800 m/s) were generated, leading to dense coatings. It was observed that the coating quality was generally compromised by the high temperature and reactivity of the small particles. To compensate for this shortcoming, the suspension feed rate was adjusted, thereby varying the thermal load on the plasma. Results showed that a slightly larger agglomerate size, in conjunction with low particle jet temperatures, could somewhat limit the decomposition of WC into brittle W_2C/W_3C and amorphous cobalt containing binder phases.

Keywords nanostructured coatings, suspension plasma spraying, tungsten-carbide cobalt

1. Introduction

WC-Co cermet coatings, produced by thermal spraying, are used extensively in industrial wear applications. Their mechanical properties are a strong function of the carbide grain size, the binder volume fraction, and the extent to which the carbides are homogeneously distributed in the binder phase. Nanostructured WC-Co coatings can potentially exhibit improved hardness, toughness, and wear resistance over conventional tungsten carbide materials when processed under optimized conditions (Ref 1). A reported increase in hardness is attributed to the decrease in grain size and reduction in the mean free path of the cobalt matrix. A fine starting powder with submicron grains favors a homogenous distribution of the carbides within the matrix and can furthermore lead to low surface roughness, requiring little additional surface finishing (Ref 2). The potential for such improvements is generating considerable interest in developing techniques for producing these coatings.

The highest hardness and wear performance of conventional tungsten carbide materials is generally obtained by those processing methods that impart high in-flight particle velocities and low particle temperatures during spraying. High particle speeds have been shown to reduce coating porosity, and low particle temperatures limit the decomposition of the carbide into brittle W_2C, W_3C, and metallic tungsten, as well as the dissolution of the cobalt binder into a weak amorphous phase. As a result, high-velocity oxyfuel (HVOF) thermal spraying has been established as a preferred method over plasma spraying (Ref 3-5). To process a nanostructured feedstock powder by HVOF, the initial cermet constituents are generally agglomerated and sintered into spherical particles of larger particle size (5-40 μm), allowing standard powder feeding (Ref 1-5).

Suspension plasma spraying using a liquid feedstock carrier is an emerging technology that permits projection of much finer starting powders directly without the need to preform and consolidate spherical feed agglomerates. In this process, a feed suspension is injected at high velocity into the plasma flame. The plasma-liquid interaction atomizes the suspension into a fine mist and evaporates the suspension medium, thereby concentrating the solid content into microsized particles. The small particles are then nearly immediately accelerated to the plasma gas velocity (Ref 6). Upon impact on the substrate, these particles form thinner lamellae than in conventional spraying (Ref 7). Thin coatings (20-100 μm) with more refined microstructures (Ref 6) and potentially smoother surface finishes are created. In spite of the high plasma temperature, the particle temperature and decomposition of the tungsten carbide material is, in principle, reduced by the evaporating liquid carrier, which imposes a substantial thermal load on the plasma. The evaporating liquid cools the forming particles and delays the onset of overheating.

In this study, the potential of this technique for consolidating nanostructured tungsten carbide cermet materials is explored. The suspension feedstock is axially injected into the center of three converging plasma streams of a Mettech Axial III plasma torch (Northwest Mettech Corp., Richmond, BC, Canada). High gas velocities, up to 1000 m/s (nearly approaching those of HVOF systems), can be generated with this torch. A procedure to prepare the liquid suspension is described. In-flight particle velocity and temperature are measured for different operating conditions of the torch, suspension feed rates, and standoff distances and are related to the resulting microstructure of the coating. Two different powder raw materials are compared, and the

This article was originally published in *Building on 100 Years of Success, Proceedings of the 2006 International Thermal Spray Conference* (Seattle, WA), May 15-18, 2006, B.R. Marple, M.M. Hyland, Y.-Ch. Lau, R.S. Lima, and J. Voyer, Ed., ASM International, Materials Park, OH, 2006.

J. Oberste Berghaus, B. Marple, and **C. Moreau,** Industrial Materials Institute, NRC, Boucherville, Québec, Canada Contact e-mail: jorg.oberste-berghaus@cnrc-nrc.gc.ca.

Table 1 Plasma operating conditions

Condition	Torch current, ×3	Gas flow, SLPM	Ar, %	N_2, %	H_2, %	Power, kW
1	200 A	245	75	10	15	83.2
2	190 A	275	75	15	10	90.1

effect of oxygen exclusion by the use of a shroud gas is investigated. Finally, possible process improvements are delineated.

2. Experimental Procedures

2.1 Spray Parameters and Material Characterization

The suspension spraying system used a Mettech Axial III plasma torch (Northwest Mettech Corp., North Vancouver, BC, Canada) equipped with an internal injection/atomization module, with nitrogen as the atomizing gas. The suspension was delivered by a positive-displacement dosing pump from an agitated reservoir and measured by a precision flow meter. By ensuring continuous flow and agitation in all wetted conduits during spraying and idle operation, sediment formation, which can cause malfunction of the solenoid valves and injector, was avoided. In an attempt to generate high particle velocities, the plasma was operated at two selected conditions with high plasma gas flow rates, as summarized in Table 1. To minimize electrode erosion, the current was adjusted to limit the torch power to ~90 kW.

In-flight particle states were measured with a commercial diagnostic system (AccuraSpray G2, Tecnar, St-Bruno, QC, Canada). The temperature measurement is based on two-color pyrometry, and velocity is determined by a time-of-flight technique. The measurement volume was centered in the spray plume at the location of the substrate during deposition, i.e., at 50 and 62.5 mm. Because the small size of the particles prevents individual in-flight particle detection, an ensemble particle diagnostic system, which senses the fluctuations of the total emitted radiation in the field of view, is deemed necessary (Ref 6).

Microstructures were observed by scanning electron microscopy (SEM) (JSM-610, JEOL, Tokyo, Japan) and field-emission scanning electron microscopy (FE-SEM) (S4700, Hitachi, Tokyo, Japan). The samples were prepared by standard metallographic methods. Porosity was assessed on the cross section by SEM (10,000×), using image analysis. Such high magnification was judged most suitable to capture the finely structured porosity in the coatings. The intensity range and thresholds were standardized on reference materials, and five measurements were averaged per sample. Vickers microhardness measurements were performed under a 300 g load for 20 s on the cross section of the coatings. Ten measurements were taken per sample at randomly selected locations.

Phase analysis was carried out by x-ray diffraction (XRD) using a Bruker D8-Discovery diffractometer (Bruker AXS, Inc., Madison, WI) with Cu Kα radiation at an acquisition of rate of 0.01°/s. The measurement is an average over a substrate area between 2 and 10 mm^2, depending on the diffraction angle. To qualitatively describe the degree of carbide degradation, two ratios of XRD reflection peak areas are defined. An index of crystallinity (IC) measures the area of crystalline peaks between 30 and 54° versus the total integrated area in this region, including

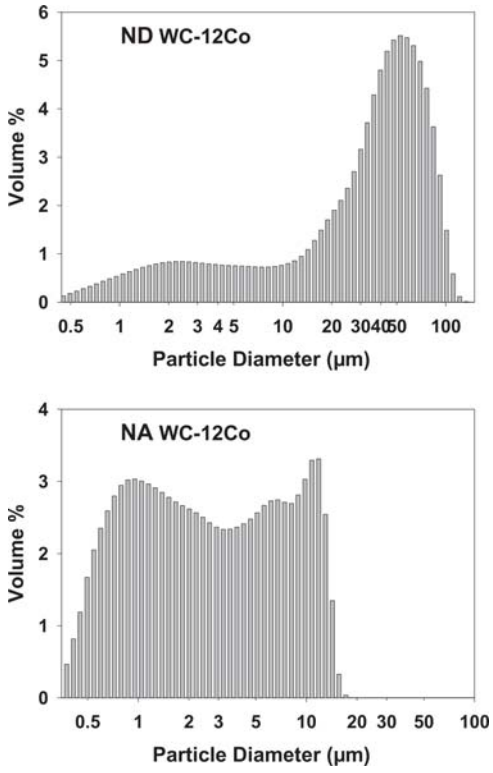

Fig. 1 Particle size distribution of feedstock powders before milling.

the diffuse amorphous hump. This index reflects the transformation of cobalt binder into a weak amorphous/η ($Co_xW_yC_z$) phase. Furthermore, an index of WC carbon compares the area of the principal WC reflection with the sum of the areas of the principal lines of all W_xC phases, including W, WC, W_2C, and W_3C. The loss of carbon is thought to occur as a result of direct oxidation on the surface of solid WC, leading to formation of non-WC phases (Ref 1). This index is an indication of the degree of oxidation of the carbides. Although these indexes do not precisely quantify the degree of degradation, they allow here an approximate comparison between the coatings obtained at different spray conditions.

2.2 Materials and Suspensions

Two different feedstock materials of WC-12% Co were used in this study, namely, a soft-agglomerated powder with a nominal carbide grain size of 60-250 nm (Nanostuctured & Amorphous Materials, Houston, TX), subsequently referred to as "NA," and an agglomerated and sintered powder with a carbide grain size 40-80 nm (formerly Nanodyne, Inc., New Brunswick, NJ), subsequently referred to as "ND." The particles of the latter material, ND, were found to disintegrate into its finer constituents. Particle size distributions of the starting powders were measured with a Coulter LS (Hialeah, FL) particle size analyzer and are shown in Fig. 1.

The morphologies and phase composition of the powders were verified by high-resolution FE-SEM and XRD, shown in the micrographs in Fig. 2 and the spectra in Fig. 3. Suspensions of 20 wt.% NA solids in ethanol (1.37 vol.%) and of 15 wt.% ND solids (1.06 vol.%) in a mixture of ethanol and 25% ethylene

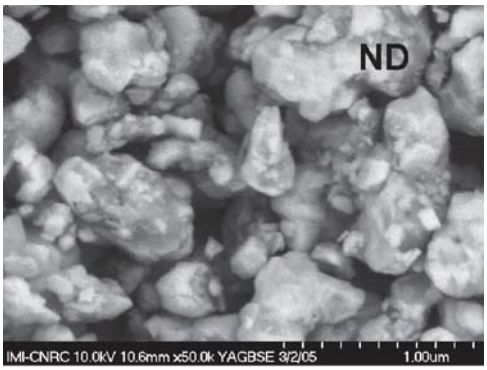

(a)

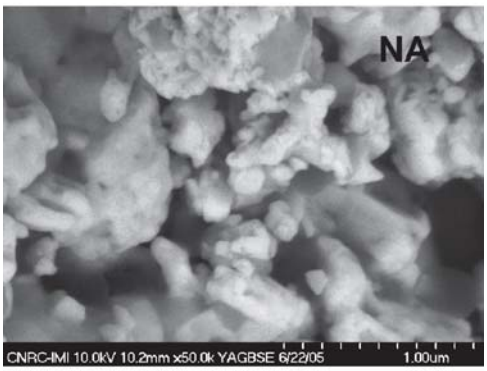

(b)

Fig. 2 Morphology of feedstock powders (a) ND and (b) NA after milling, showing angular submicron carbide constituents

glycol were prepared. The addition of the viscous glycol (b.p. 200 °C) is expected to stabilize the suspension and impose an additional thermal load on the plasma during spraying.

The high specific density of WC-Co powders and the widely different acid/base properties of the two main particulate constituents (WC, or rather the surface oxide WO_3, is a Lewis acid and CoO is basic) make this system difficult to disperse in a suspension. Polyethyleneimine (PEI) (MW 25,000, Alfa Aesar, Ward Hill, MA) was used as dispersing agent. This cationic polyelectrolyte adsorbs onto the tungsten oxide surfaces and can be charged positively by protonation of the amine groups, i.e., by adjusting the pH to less basic conditions (Ref 8). Care must be taken not to add too much acid in the pH adjustment and thereby cause dissolution of cobalt according to the reaction $CoO + H_2O \leftrightarrow Co^{2+} + 2OH^-$, which increases the pH and thereby effectively buffers the system (Ref 9). Suspensions were prepared in ethanol by mixing 80 wt.% powder, PEI (0.6 wt.% per solids), and an appropriate amount of WC grinding balls in a 2 L polyethylene milling jar. Milling was needed to break down the particle agglomerates and was performed at a speed of 140 rpm for 24 h. After washing of the ball mill and medium, the pH was immediately adjusted by addition of 1 M HCl to a final value between pH 8 and 9, at which point the solution starts buffering, i.e., no further decrease in pH was possible by acid addition. The effectiveness of the milling procedure, dispersing agent, and pH adjustment was qualitatively assessed by sedimentation tests. The procedure outlined above stabilized the dispersion sufficiently to be compatible with the spray process. Addition of viscous ethylene glycol, as in the case of the ND feedstock, further prolonged the settling time of the suspension.

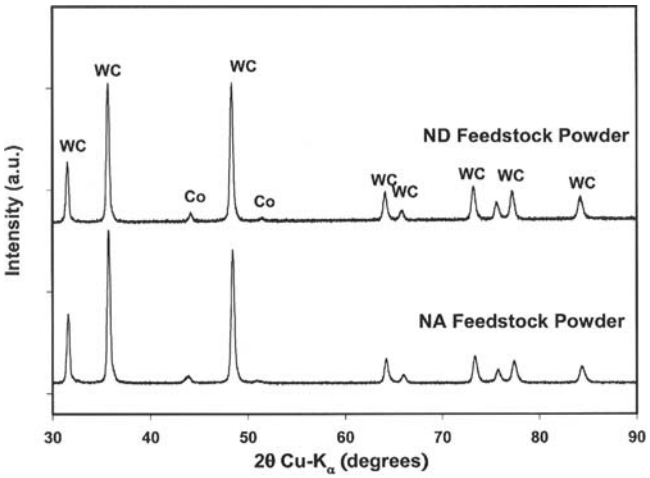

Fig. 3 XRD spectra of feedstock powders

2.3 Substrate Considerations

Coatings were produced on mild steel substrates with dimensions of 25 × 75 × 12.5 mm. To increase coating adhesion, the substrate surface was grit-blasted with 60 grit Al_2O_3 particles prior to deposition. Initially, high substrate temperatures provoked oxidation of the coating surface after each torch pass and led to detachment of each subsequent layer. Backside cooling of the substrate using both compressed air and water was consequently implemented. Compressed air cooling on the front surface of the substrate, i.e., where the coating is deposited, was observed to deflect the particle jet issuing from the torch and posed the risk of adversely affecting the resulting coating. Attempts were made to reduce the cooling air jet flow while maintaining a surface temperature not exceeding 200 °C.

3. Results and Discussion

3.1 Processing Conditions and Particle States

The effect of processing conditions was mainly assessed on the 20 wt.% NA (WC-12Co) suspension in ethanol. Measured particle states for selected operating conditions of varying plasma gas flow, suspension flow rate, and standoff distance are summarized in Table 2.

With an increase in gas flow rate (plasma condition 2), particle velocities up to 800 m/s could be generated. Such high velocities are rarely attained in atmospheric plasma spraying. The high particle velocities are the result of the small particle size and high gas velocity. The small particles have been shown to intimately follow the gas flow velocity as they are entrained in the plasma stream (Ref 6). However, this particle speed is rapidly lost at increasing spray distance, as seen from the measurement at 62 mm standoff. Previous work has shown that the impact velocities on the substrate are reduced from the free stream values but scale strongly with free stream conditions (Ref 6).

High average particle temperatures between 2180 and 2440 °C were measured. For optimized HVOF spray conditions, using 5-40 μm feed agglomerates, particle temperatures are usually much lower (1600-2000 °C) but are reported to increase

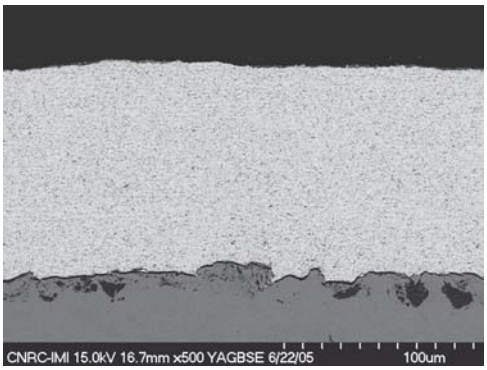

Fig. 4 Cross-section micrograph for coating NA-2

Table 2 Particle states at selected spray conditions for plasma settings from Table 1(a)

Sample	Plasma condition	Susp. FR, kg/h	SD, mm	$V_{part.}$, m/s	$T_{part.}$, °C
NA-1	1	3.6	50	714	2179
NA-2	1	2.5	50	706	2254
NA-3	1	1.5	50	737	2432
NA-4	2	2.5	50	790	2293
NA-5-SD(b)	1	2.5	62	642	2279
NA-6-SD(b)	2	3.5	62	754	2261
NA-7-SH(c)	1	2.5	114	277	2439
ND-1	1	3.0	50	608	2202

(a) FR, feed rate; NA, nanostructured and amorphous materials; ND, nanodyne. (b) SD, spray distance at 62 mm. (c) SH, gas shroud installed

with decreasing particle size (Ref 1). The much smaller particle sizes, generated from the suspension, likely govern the attainable temperature range. Nonetheless, particle temperatures were reduced from 2432 to 2180 °C by increasing the suspension feed rate from 1.5 to 3.5 kg/h (see NA-3 to NA-1). Concurrently, particle speeds of ~700 m/s were maintained. The lowest temperature was also obtained by changing the suspension carrier to a high boiling point medium, such as ethylene glycol (ND-1), using a high feed rate. The total thermal load on the plasma is thereby used as an independent tuning parameter for the particle temperature. It should be mentioned that the use of a slightly larger torch exit nozzle for the ND-1 sample explains the lower particle velocity of 600 m/s.

3.2 Coating Structure and Phase Composition

The microstructures of the coatings are shown in Fig. 4 and 5. Depending on the operating conditions and the feeding rates, deposition rates varied from ~1.3 to 2.8 μm/pass. A pass constitutes a scan pattern of the torch covering the entire area of the substrate. Coatings up to 150 μm thick were produced. The initial layers of the coating filled the original surface features of the grit-blasted substrate, resulting in a final surface roughness of $R_a < 3$ μm, as measured with a profilometer. This roughness is sufficient for some industrial applications, or if finishing steps are needed, polishing is likely facilitated over conventional WC-Co coatings (Ref 3).

Coating porosities varied from 9 to <0.2%. The low porosity comes, however, at the expense of substantial degradation of the WC-Co. XRD spectra of the coatings in Fig. 6 reveal a strong

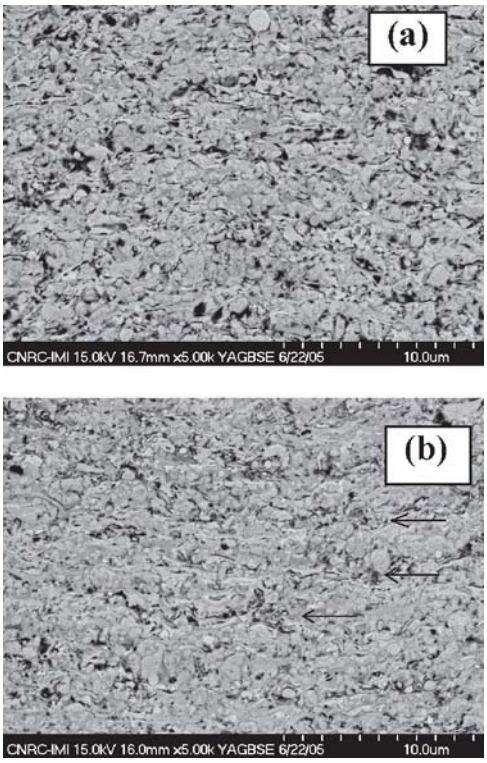

Fig. 5 Microstructures of (a) NA-2 and (b) NA-4

presence of W_2C, W_3C, and even metallic W, as well as a characteristic amorphous "hump" in the region of 35-54°. Some decomposition of small WC grains in thermal spraying is usually reported and is attributed to the increased reactivity of the fine carbide particles (Ref 1, 3). In addition, the agglomerate particles created from the suspension are much smaller than for conventional spraying, further elevating surface reactivity.

3.3 Microstructure, Composition, and Mechanical Properties

Mechanical properties of WC-Co coatings, such as hardness, strongly depend on both the porosity and the quality of carbide after processing (Ref 1). Indices of crystallinity and WC carbon content are summarized in Fig. 7, and porosity values for the selected coatings are shown in Fig. 8. The hardness values, determined for these coatings, are shown in Fig. 9.

Distinct carbide degradation in terms of a decrease in WC carbon content and a low degree of crystallinity for samples NA-1 through NA-3 are observed in Fig. 7. As explained above, the samples were formed at particle temperatures increasing from 2180 to 2430 °C at similar particle velocity. Although the sample obtained with the hottest particles (NA-3) shows very low porosity values (<0.2%), its hardness decreased substantially. The higher particle temperature not only increases the reactivity of the surface for oxidation but also fosters more rapid dissolution of the fine-scale WC grains into the liquid metal during spraying (Ref 3). The microstructure in Fig. 10(a), for example, shows only few angular-shaped carbide constituents and is dominated by rounded and deformed features, which have likely undergone degradation. The corners and edges of the car-

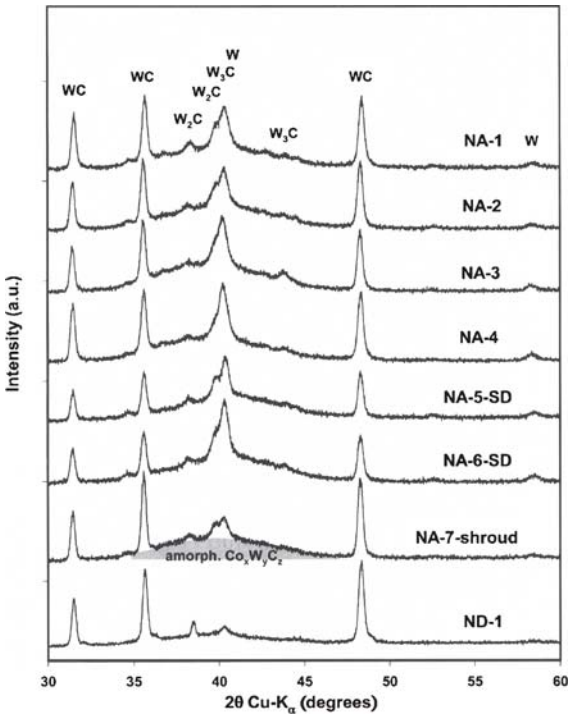

Fig. 6 XRD spectra of selected coatings

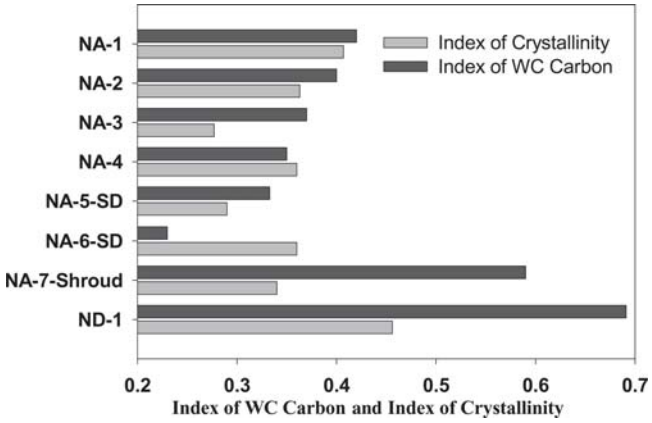

Fig. 7 Summary XRD analysis, index of WC carbon, and index of crystallinity

bide are more readily dissolved because of the added reactive contact area to the cobalt.

The effect of coating porosity on microhardness is illustrated by comparing samples NA-2 and NA-4. These samples were produced at similar particle temperature (2250 °C) but different particle velocity, i.e. 700 and 790 m/s. With increasing velocity, a densification from 1.5 to <0.2% porosity was induced (Fig. 8). The decreased porosity resulted in one of the harder coatings (~700 $HV_{0.3}$) of this study.

An increase in spray distance from 50 to 62 mm resulted in a softer coating for both plasma conditions (conditions 1 and 2). Sample NA-5-SD has higher porosity and a lower hardness than the corresponding sample NA-2. A similar trend can be seen by comparing NA-6-SD to NA-4. In both cases, a drop in particle

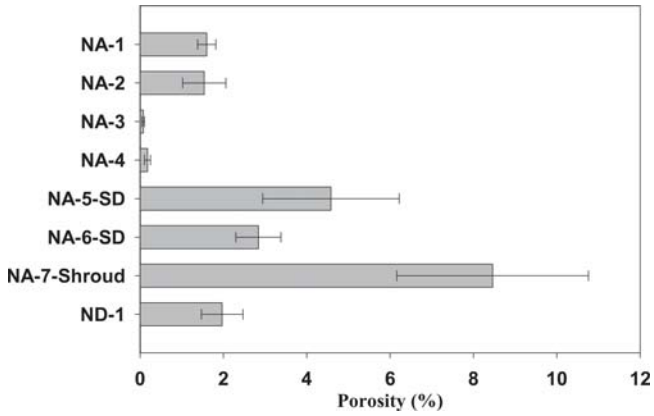

Fig. 8 Porosity values for selected coatings from SEM image analysis (original magnification, 10,000×)

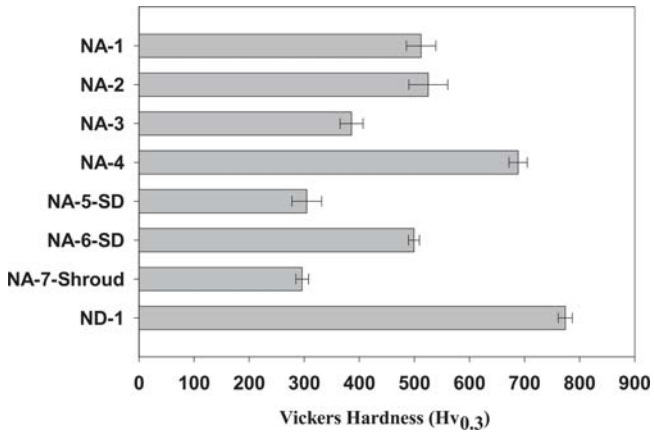

Fig. 9 Hardness $HV_{0.3}$ for selected samples

velocity was measured. Furthermore, the coatings obtained at larger standoff distances were more degraded and oxidized (Fig. 7, 8, and 9).

It is interesting to note that the deposits obtained at condition 2, i.e., at higher jet velocities (NA-4 and NA-6-SD), show a lower WC carbon index than those at condition 1 (NA-2 and NA-5-SD), even though they have an equal or higher degree of crystallinity. At high particle velocities, very small particles, even those that travel on the periphery of the principal particle jet, may be incorporated into the coating. Those particles, in turn, are most likely to be oxidized, due to their proximity to the surrounding air and to their elevated surface reactivity. At lower velocity, the very small particles are prevented from reaching the substrate because they are entrained in the radially deflecting gas flow in front of the substrate (Ref 6). Layers of oxidized particles can be identified in the microstructure of those coatings (Fig. 4 and 5b, see arrows), appearing as dark strata in the back-scattered electron image. The arrows in Fig. 5 indicate some of these darker strata. EDX measurements confirmed higher oxygen content in the dark strata as compared with the bordering lighter layers. A coating layer is formed at each pass of the torch, following a raster pattern and covering the adjacent layers with the oxidized particles. Oxidation of the exposed top surface of the coating after each pass may also play a role.

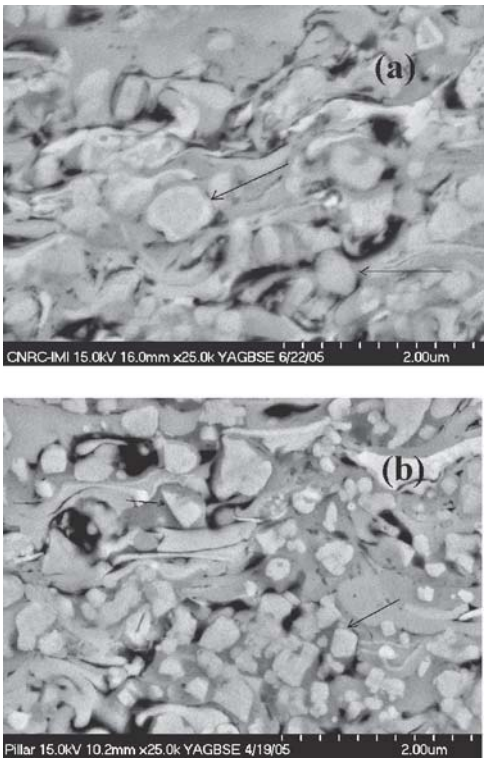

Fig. 10 Microstructure of samples (a) NA-4 and (b) ND-1

The use of an argon shroud, shielding the plasma and particle jet from air entrainment, resulted in a substantial reduction in oxidation. A high index of WC carbon is measured in the resulting coating (NA-7-Shroud in Fig. 7). However, the shroud attachment necessitates large spray distances, and the radial argon jet disturbed the plasma flow, leading to low particle velocities and high particle temperatures. The coatings have very high porosities, low crystallinity, and, consequently, low hardness values.

The hardest coating in this study was obtained with the Nanodyne powder (ND-1) suspended in an ethanol/ethylene-glycol carrier. The high boiling point medium, in conjunction with a high feed rate, was anticipated to reduce the in-flight particle temperatures and delay the onset of overheating of the small particles while stabilizing the suspension. Indeed, the highest index of crystallinity and WC carbon content were measured for this coating, as seen in Fig. 7. The microstructure, shown in Fig. 10(b), reveals a higher number of angular carbides, as indicated by the arrows. Also, the degree of oxidation in this coating is reduced. A more agglomerated feedstock, even after ball milling, may have led to less dispersion of submicron particles by the plasma flame or may have lowered the reactivity of the particles. A lesser degree of atomization of the viscous glycol mixture may also reduce the amount of overspray oxides deposited. Because of the relatively low particle velocity of only 600 m/s, ND-1 is not the densest coating in this study. An additional increase in hardness could be expected at higher velocities.

Ultimately, the obtained hardness values in this preliminary study are far below the values reported in the literature for both conventional (Ref 1) and nanostructured WC-Co coatings (Ref 3-5) sprayed by HVOF, which are on the order of 1000-1550 $Hv_{0.3}$. On the other hand, suspension spraying showed the potential to produce very dense coatings with a relatively smooth surface finish. The principal obstacle is the high reactivity of the small particles, which degrade easily during the spray process. Careful adjustments of the spray conditions and feedstock preparation are possible avenues for reducing particle temperature, carbide degradation, and oxide deposition and thereby improving coating properties.

4. Conclusions

- The potential of suspension plasma spraying as a novel method for the consolidation of nanostructured WC-Co coatings is explored. The high particle velocities, the small splat sizes, and the possible control of the particle temperature make this technique a promising candidate.
- Coating hardness is a strong function of porosity and degree of carbide degradation. Porosity was decreased to <0.2% with increasing particle velocities up to 800 m/s.
- The degree of degradation of carbides and binder into amorphous phases is reduced at lower particle temperature. Lower temperatures are induced by varying the suspension feed rate and increasing the total thermal load. Because of the small particle size, however, temperatures below 2200 °C could not be produced.
- The measured carbon loss in the carbide is principally associated with deposition of layers of highly oxidized overspray.
- The properties of the feedstock powder and feed suspension play a critical role in carbide quality in the resulting coating.
- The principal limitations to produce coatings of comparable hardness to those from established technologies were identified to be the high reactivity of the small particles during spraying, leading to degradation and oxidation of the carbide phase.

References

1. J. He and J.M. Schoenung, A Review on Nanostructured WC-Co Coatings, *Surf. Coat. Technol.,* 2002, **157,** p 72-79
2. F. Fischer, M.D. Dvorak, and S. Siegmann, Development of Ultra Thin Carbide Coatings for Wear and Corrosion Resistance, *Thermal Spray 2001: New Surfaces for a New Millennium* (Singapore), C.C. Berndt, K.A. Khor, and E.F. Lugscheider, Ed., ASM International, 2001, p 1131-1135
3. D.A. Stewart, P.H. Shipway, and D.G. McCarteny, Abrasive Wear Behaviour of Conventional and Nanocomposite HVOF-Sprayed WC-Co Coatings, *Wear,* 1999, **225-229,** p 789-798
4. J. Voyer and B.R. Marple, Thermal Spray Processing of WC-Co Nanomaterials, *Thermal Spray: Surface Engineering via Applied Research,* C.C. Berndt, Ed., May 8-11, 2000 (Montréal, Québec, Canada), ASM International, 2000, p 895-904
5. B.R. Marple and R.S. Lima, Process Temperature/Velocity-Hardness-Wear Relationships for High-Velocity Oxyfuel Sprayed Nanostructured and Conventional Cermet Coatings, *J. Therm. Spray Technol.,* 2005, **14**(1), p 67-76
6. J. Oberste Berghaus, S. Bouaricha, J.-G. Legoux, and C. Moreau, Suspension Plasma Spraying of Nanoceramics Using an Axial Injection Torch, *Thermal Spray Connects: Explore Its Surfacing Potential,* E. Lugscheider and C.C. Berndt, Ed., May 2-4, 2005, 2005 (Basel, Switzerland), ASM International
7. P. Fauchais, Understanding Plasma Spraying, *J. Phys. D, Appl. Phys.,* 2004, **37,** p R86-R108
8. E. Laarz and L. Bergström, Dispersing WC-Co Powders in Aqueous Media with Polyethylenimine, *Int. J. Refract. Met. Hard Mater.,* 2000, **18,** p 281-286
9. K.M. Andersson and L. Bergström, Aqueous Processing of WC-Co Powders: Suspension Preparation and Granule Properties, *Ceram. Trans., Colloid. Ceram. Process.,* 2004, **152,** p 93-107